

## Critical Capacitance and Charge-Vortex Duality Near the Superfluid-to-Insulator Transition

Snir Gazit, Daniel Podolsky, and Assa Auerbach

*Physics Department, Technion-Israel Institute of Technology, 32000 Haifa, Israel*

(Received 3 July 2014; published 8 December 2014)

Using a generalized reciprocity relation between charge and vortex conductivities at complex frequencies in two space dimensions, we identify the capacitance in the insulating phase as a measure of vortex condensate stiffness. We compute the ratio of boson superfluid stiffness to vortex condensate stiffness at mirror points to be 0.21(1) for the relativistic O(2) model. The product of dynamical conductivities at mirror points is used as a quantitative measure of deviations from self-duality between charge and vortex theories. We propose the finite wave vector compressibility as an experimental measure of the vortex condensate stiffness for neutral lattice bosons.

DOI: 10.1103/PhysRevLett.113.240601

PACS numbers: 05.60.Gg, 05.30.Jp, 05.30.Rt, 37.10.Jk

Two dimensional superfluid-to-insulator transitions (SIT) have been observed in diverse systems, e.g., Josephson junction arrays [1], cold atoms trapped in optical lattices [2–4], and disordered superconducting films [5]. Recent experiments have uncovered important dynamical properties near the quantum critical point: a softening amplitude (Higgs) mode observed in the optical lattice [4], and a critically suppressed threshold frequency seen by terahertz conductivity in superconducting films [6]. These have motivated numerical studies of real-time correlations near criticality [7–9], and novel ideas from holography [10–12].

Three decades ago, Fisher and Lee [13] showed that the SIT can be described as the Bose condensation of quantum vortices. Despite the appeal of this description,  $\rho_v$ , the vortex condensate stiffness, has remained an elusive observable, for which no experimental probe has yet been proposed. Also, to our knowledge,  $\rho_v$  has not been calculated near the critical point, for any microscopic model.

In this Letter, we address this problem, by using an exact reciprocity relation between complex dynamical conductivities of bosons ( $\sigma$ ) and vortices ( $\sigma_v$ )

$$\sigma(\omega) \times \sigma_v(\omega) = q^2/h^2, \quad (1)$$

where  $q$  is the boson charge ( $= 2e$  in superconductors) [14]. At low frequencies, this equation is dominated by the reactive (imaginary) conductivities. The superfluid stiffness  $\rho_s$  in the superfluid (sf) phase can be measured by the low frequency inductance  $L_{sf}$ ,  $\rho_s = \hbar/(2\pi\sigma_q L_{sf})$ , where  $\sigma_q = q^2/h$  is the quantum of conductance. Equation (1) allows us to identify the elusive vortex condensate stiffness with the capacitance per square in the insulating phase,  $C_{ins} = \hbar\sigma_q/(2\pi\rho_v)$ .

The charge-vortex duality (CVD) is an exact mapping between boson and vortex degrees of freedom near the SIT.

In the presence of particle hole symmetry, the CVD is mathematically equivalent to the well known classical statistical mechanics duality mapping between the XY model and a lattice superconductor in three space dimensions [15,16]. A related, but distinct, concept to CVD is self-duality, a property of certain physical systems in which the original and dual degrees of freedom satisfy identical dynamics. If the CVD mapping were self-dual then the universal critical conductivity at the SIT would equal exactly  $\sigma_q$  [13]. Experiments, however, have measured nonuniversal values of the critical conductivity [5], indicating that the boson and vortex theories are not self-dual. This is attributed mainly to the different interaction ranges of bosons (in the superfluid) and vortices (in the insulator). Moreover, in real experiments, several additional factors

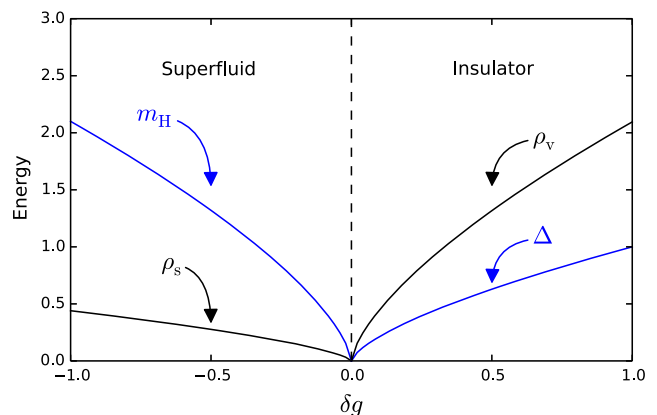


FIG. 1 (color online). Critical energy scales near the SIT computed by QMC calculations. The superfluid is characterized by the mass of the amplitude mode,  $m_H$ , and the superfluid stiffness,  $\rho_s$ , the insulator by the single particle gap,  $\Delta$ , and the vortex condensate stiffness,  $\rho_v$ . The amplitude ratios  $m_H(-\delta g)/\Delta(\delta g) = 2.1(3)$  [17],  $\rho_s(-\delta g)/\Delta(\delta g) = 0.44(1)$  [7], and  $\rho_v(\delta g)/\Delta(\delta g) = 2.1(1)$  are universal.

can spoil self-duality: (i) potential energy (both confining and disordered), which couples differently to charges and vortices and (ii) fermionic (Bogoliubov) quasiparticles in superconductors produce dissipation, which can alter the phase diagram from the purely bosonic theory.

In a self-dual theory, one expects  $\rho_s(-\delta g) = \rho_v(\delta g)$ , where  $\pm\delta g$  are mirror points on either side of the SIT. Figure 1 depicts all the critical energy scales of the relativistic O(2) field theory, obtained by large-scale Monte Carlo simulation. In addition to the Higgs mass  $m_H$  and the charge gap  $\Delta$ , which vanish at the critical point, we compare the energy scales  $\rho_s$  and  $\rho_v$  which are also critical, but have different relative amplitudes. The ratio  $\rho_s(-\delta g)/\rho_v(\delta g) = 0.21(1)$  differs from unity and, hence, quantifies the deviation from self-duality.

It is interesting to ask whether self-duality is better satisfied at finite frequencies. To address this, we propose the product function

$$\mathcal{R}(z) \equiv \sigma(z, -\delta g) \times \sigma(z, \delta g) / \sigma_q^2, \quad (2)$$

as a measure of self-duality between mirror points. Here,  $z$  denotes either a real or a Matsubara frequency.

The high frequency conductivity [18] (after removal of cutoff dependent corrections) reaches a universal value  $\sigma^* = 0.355(5)\sigma_q$  [10,11]. We compute the function  $\mathcal{R}(i\omega_m)$  and address its implications to CVD. We conclude by proposing an experimental measure of the vortex condensate stiffness  $\rho_v$  for neutral bosons in an optical lattice.

*Vortex transport theory.*—Boson charge current  $\vec{j}$  is driven by an electrochemical field  $\vec{E}$ . Vortices are point particles in two dimensions. The vorticity current  $\vec{j}_v(t)$  is driven by the Magnus field  $\vec{E}_v$ . Hydrodynamics dictate simple relations between electrochemical field and vortex number current, and between boson charge current and Magnus field [19]

$$E_v^\alpha = \frac{\hbar}{q} \epsilon^{\alpha\beta} j^\beta, \quad E^\alpha = \frac{\hbar}{q} \epsilon^{\alpha\beta} j_v^\beta, \quad (3)$$

where  $\epsilon = i\sigma^y$  is the two dimensional antisymmetric tensor. We note that Eqs. (3) are instantaneous. Conductivity relates currents to their driving fields

$$j_{(v)}^\alpha(t) = \int_{-\infty}^t dt' \sigma_{(v)}^{\alpha\beta}(t-t') E_{(v)}^\beta(t'). \quad (4)$$

By Fourier transformation, the complex dynamical conductivities obey a reciprocity relation  $\epsilon^\top \sigma_v \epsilon = (q^2/\hbar^2) \sigma^{-1}$ . For the case of an isotropic longitudinal conductivity  $\sigma^{xx} = \sigma^{yy} = \sigma$ , one obtains the reciprocity Eq. (1), which can be analytically continued to Matsubara space  $\omega \rightarrow i\omega_n$ .

*Model and observables.*—For numerical simulations, we study the discretized partition function

$\mathcal{Z} = \int \mathcal{D}\varphi \mathcal{D}\varphi^* e^{-S[\varphi, \varphi^]}$ , where the real action  $S$  on Euclidean space-time is

$$S = \sum_{(i,j)} \varphi_i \varphi_j^* + \text{c.c.} + 2\mu \sum_i |\varphi_i|^2 + 4g \sum_i |\varphi_i|^4. \quad (5)$$

Here,  $\varphi_i$  are complex variables defined on a cubic lattice of size  $L \times L \times \beta$ . We take  $\beta = L$  throughout. For  $\mu < 0$ , this model undergoes a continuous zero temperature quantum phase transition (QCP) between a superfluid with  $\langle \varphi \rangle \neq 0$  for  $g < g_c$  and an insulator with  $\langle \varphi \rangle = 0$  for  $g > g_c$ . We define the quantum detuning parameter  $\delta g = (g - g_c)/g_c$ .

The critical energy scales near the SIT, as shown in Fig 1, in the superfluid phase are the amplitude mode mass  $m_H$  and the superfluid stiffness  $\rho_s$  [17,20]. In the insulating phase, excitations are gapped, with single-particle gap  $\Delta$ .

The lattice current field is  $J_{i,\eta} = -(\delta S/\delta A_{i,i+\eta})$ , where we have introduced a  $U(1)$  lattice gauge field by Peierls substitution  $\varphi_i \varphi_j^* \rightarrow \varphi_i \varphi_j^* e^{iA_{i,i+\eta}}$ . The dynamical conductivity is given by the current-current correlation function

$$\begin{aligned} \tilde{\sigma}(\omega_m) &= -\frac{\Pi_{xx}(\omega_m)}{\omega_m}, \\ \Pi_{xx}(\omega_m) &= \frac{1}{L^2 \beta} \sum_{i,j} e^{i\omega_m \tau_{ij}} \frac{\delta \langle J_{i,x} \rangle}{\delta A_{j,x}}, \end{aligned} \quad (6)$$

where  $\omega_m = 2\pi mT$  is a Matsubara frequency and  $\tau_{ij}$  is the discrete imaginary time interval between points  $i, j$ . Remarkably, in  $2+1$  dimensions, the conductivity has zero scaling dimension [14], such that it is given by a universal amplitude with scaling form

$$\tilde{\sigma}(\omega_m) = \sigma_q \Sigma_{\pm}(\omega_m/\Delta), \quad (7)$$

where  $\Sigma_+$  ( $\Sigma_-$ ) belongs to the insulating (superfluid) phase. Real frequency dynamics can be obtained by analytic continuation  $\sigma(\omega) = \tilde{\sigma}(\omega_m \rightarrow -i\omega + 0^+)$ .

In the superfluid phase, the reactive conductivity diverges as  $\text{Im}[\sigma_{\text{sf}}(\omega)] = 2\pi\sigma_q\rho_s(-\delta g)/(\hbar\omega)$ . Previous calculations [21] show that the dissipative component has a small subgap contribution below the Higgs mass,  $0 < \omega \ll m_H(-\delta g)$  which goes as  $\text{Re}[\sigma_{\text{sf}}(\omega)] \sim \omega^5$ . This is negligible as  $\omega \rightarrow 0$  and the analytic continuation to Matsubara frequency yields

$$\tilde{\sigma}_{\text{sf}}(\omega_m) \sim \frac{2\pi\sigma_q\rho_s}{\hbar\omega_m}, \quad (\text{for } \omega_m \ll m_H). \quad (8)$$

In the insulator (ins), the dissipative conductivity vanishes identically below the charge gap  $\Delta(\delta g)$  [7,22]. The reactive conductivity vanishes linearly with frequency  $\text{Im}[\sigma_{\text{ins}}(\omega)] = -C_{\text{ins}}\omega$ , where  $C_{\text{ins}}$  is the capacitance per square. As a result, the conductivity, as a function of the complex frequency  $z$ , has a radius of convergence of  $2\Delta$  about  $z = 0$  and in the low frequency limit, it is given by

$\sigma_{\text{ins}} = -iCz$ . This can be analytically continued to Matsubara space by setting  $z = i\omega_m$ , which yields

$$\tilde{\sigma}_{\text{ins}}(\omega_m) \sim C_{\text{ins}}\omega_m, \quad (\text{for } \omega_m \ll \Delta). \quad (9)$$

Equation (7) implies that the capacitance  $C_{\text{ins}}$  diverges near the QCP as  $C_{\text{ins}} \sim 1/\Delta$ . The capacitance measures the dielectric response of the insulator. Its divergence reflects the large particle-hole fluctuations near the transition.

In the vortex description, the insulator is a bose condensate of vortices, with a low frequency vortex conductivity  $\tilde{\sigma}_v(\omega_m) = \rho_v/(\hbar^2\omega_m)$ . As a consequence,  $\rho_v$  can be defined in terms of the capacitance by applying Eq. (1)

$$\rho_v \equiv \frac{\hbar\sigma_q}{2\pi C_{\text{ins}}}. \quad (10)$$

We shall use this important relation to test for self-duality in the 2 + 1 dimensional O(2) field theory.

*Methods.*—A large scale quantum Monte Carlo (QMC) simulation of Eq. (5) is used to evaluate Eq. (6). To suppress the effect of critical slowing down near the phase transition we use the classical worm algorithm [23]. This method samples closed loop configurations of a dual integer current representation of the partition function. This enables us to consider large systems, of linear size up to  $L = 512$ , which is crucial for obtaining universal properties. To validate the universality of our results, we performed our analysis on two distinct crossing points of the SIT, by choosing  $\mu = -0.5$  and  $\mu = -5.89391$  and tuning  $g$  across the transition. We found excellent agreement within the error bars. Henceforth, we will only present results for  $\mu = -5.89391$ , a value which has been argued to reduce finite size corrections to scaling [24].

First, we locate the critical coupling  $g_c(\mu)$  with high accuracy. This can be achieved by a finite size scaling analysis of the superfluid stiffness  $\rho_s = (1/L)(\partial\mathcal{Z}(\varphi)/\partial\varphi)|_{\varphi=0}$  [25], where  $\mathcal{Z}(\varphi)$  is the partition function in the presence of a uniform phase twist  $\varphi$ . In this work, we find  $g_c = 7.0284(3)$ .

We extract the gap  $\Delta$  in the insulator by analyzing the asymptotic large imaginary time decay of the two point Green's function. In a gapped phase, this has an exponential decay of the form  $G(\tau) \sim e^{-\Delta\tau} + e^{-\Delta(\beta-\tau)}$ , where  $\beta = 1/T$ . We compute  $\Delta$  by a fit to this form. Near criticality, the gap is expected to scale as a power law  $\Delta = \Delta_0|\delta g|^\nu$ , where  $\nu$  is the correlation length exponent. We use  $\nu = 0.6717(3)$ , as obtained by previous high accuracy Monte Carlo studies of the 3D XY model [26]. Our results for  $\Delta(\delta g)$  are in excellent agreement with the expected scaling, with the nonuniversal prefactor  $\Delta_0 = 2.09(5)$ .

*Results.*—In Fig. 2, we present the dynamical conductivity  $\sigma(\omega_m)$  as a function of Matsubara frequency, both in the insulator and in the superfluid, for a range of detuning parameters  $\delta g$  near the critical point. To suppress finite size

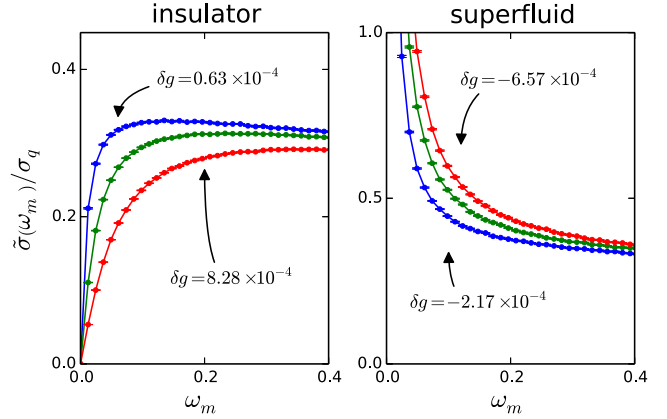


FIG. 2 (color online). The conductivity as a function Matsubara frequency. The curves differ by the detuning parameter  $\delta g$ . In the insulator, the low frequency conductivity is linear,  $\sigma_{\text{ins}} \sim \omega_m$  indicating capacitive behavior. In the superfluid, the conductivity diverges as  $\sigma_{\text{sf}} \sim 1/\omega_m$  indicating inductive response.

effects in the insulator, we used an improved estimator, in which we consider only loop configurations with zero winding number [10,11]. We find that the dynamical conductivity as a function of  $\omega_m$  in Fig. 2, follows the form of the low frequency reactive conductivity both in the superfluid, Eq. (8), and in the insulator, Eq. (9).

Next, we calculate  $\rho_s$  and  $\rho_v$  in their respective phases. The superfluid stiffness  $\rho_s$  was calculated using the standard method of winding number fluctuations [27]. In order to extract  $\rho_v$ , we use the relation in Eq. (10). As a concrete Monte Carlo observable for the capacitance, we use the conductivity evaluated at the first nonzero Matsubara frequency

$$C(\delta g) = \lim_{L \rightarrow \infty} \frac{\sigma(\omega_m = \frac{2\pi}{L}, \delta g)}{\frac{2\pi}{L}}. \quad (11)$$

Both the vortex condensate stiffness  $\rho_v$  and the superfluid stiffness  $\rho_s$  near the critical point follow a power law behavior  $\rho_{\{s,v\}} \sim \rho_{\{s,v\}}^0 |\delta g|^\nu$ . The nonuniversal prefactors  $\rho_v^0$  and  $\rho_s^0$  are extracted by a numerical fit. We find  $\rho_s/\rho_v = 0.21(1)$ . Finite size scaling effects are discussed in the Supplemental Material [28]. Surprisingly, this value is close to the value  $\rho_s/\rho_v = 0.23$  obtained by a simple one loop weak coupling calculation [7].

The universal scaling function of the dynamical conductivity is obtained by rescaling the Matsubara frequency axis by the single particle gap  $\Delta$ . Curves for different detuning parameters  $\delta g$  collapse into a single universal curve at low frequencies. On the other hand, at high frequencies,  $\omega_m$  need not be a negligible fraction of the UV cutoff scale  $\Lambda$ . This leads to nonuniversal corrections in the conductivity that depend on powers of  $\omega_m/\Lambda$ . We take these into account by fitting the numerical QMC data to the following scaling form:

$$\sigma_{\pm}(\omega_m, \delta g, \Lambda) = \sigma_q \Sigma_{\pm} \left( \frac{\omega_m}{\Delta} \right) + A \frac{\omega_m}{\Lambda} + B \left( \frac{\omega_m}{\Lambda} \right)^2. \quad (12)$$

Here,  $A$  and  $B$  are expected to depend smoothly on the detuning parameter  $\delta g$ . Since we consider a narrow range of values of  $\delta g$ , we approximate  $A$  and  $B$  as constants. This enables us to extract the universal functions  $\Sigma_{\pm}$  on both phases by using only two fitting parameters. For further details, see the Supplemental Material [28].

The result of this analysis is shown in Fig. 3(a), where we subtract the nonuniversal part of the conductivity using Eq. (12). The conductivity curves, on each side of the phase transition, collapse, with high accuracy, to the universal conductivity functions  $\Sigma_{\pm}(\omega_m/\Delta)$ .

At high frequencies, the universal conductivity curves saturate to a plateau, with  $\sigma(\omega \gg \Delta) = 0.354(5)\sigma_q$  in the insulating phase and  $\sigma(\omega \gg \Delta) = 0.355(5)\sigma_q$  in the superfluid phase. As a result, we conclude that the high frequency universal conductivity,  $\sigma^*$ , is a robust quantity across the phase transition. Our scaling correction analysis differs significantly from that of Refs. [10–12], yet the value of the high-frequency conductivity is in agreement with their results.

Finally, we study deviations from self-duality as a function of Matsubara frequency. In Fig. 3(b), we depict the product of the Matsubara frequency conductivity evaluated at mirror points across the critical point,  $\mathcal{R}(\omega_m) = \sigma(\omega_m, \delta g)\sigma(\omega_m, -\delta g)/\sigma_q^2$ . In order to study the critical properties, we subtract the nonuniversal cutoff corrections. Note that, for  $\omega_m \gg \Delta$ ,  $\mathcal{R} \rightarrow (\sigma^*/\sigma_q)^2$ , whereas for  $\omega_m \ll \Delta$ ,  $\mathcal{R}$  approaches the product of reactive conductivities in the two phases. In both limits, the Matsubara and real frequency results coincide,  $\mathcal{R}(\omega) = \mathcal{R}(\omega_m)$ . By contrast, at intermediate frequencies, determination of  $\mathcal{R}(\omega)$  requires analytical continuation. If the CVD were self-dual, then Eq. (1) would imply that this product is frequency independent and equal to 1. Our results display a nontrivial frequency dependence and deviate from the predicted self-dual value. We attribute this deviation to the different interaction range of charges and vortices.

*Discussion and summary.*—The universal ratio of the reactive conductivities  $C_{\text{ins}}/L_{\text{sf}}$  motivates future experiments as it provides a direct probe of the charge-vortex duality.

Recent THz spectroscopy measured the complex ac conductivity near the SIT in superconducting InO and NbN thin films [6]. In these systems, the superfluid stiffness in the superconducting phase can be measured from the low frequency reactive response [32,33]. Detecting the diverging capacitance in the insulating side may require careful subtraction of substrate signal background [34].

Another experimental realization of the SIT is the Mott insulator-to-superfluid transition of cold atoms trapped in an optical lattice. At integer filling, the transition has an

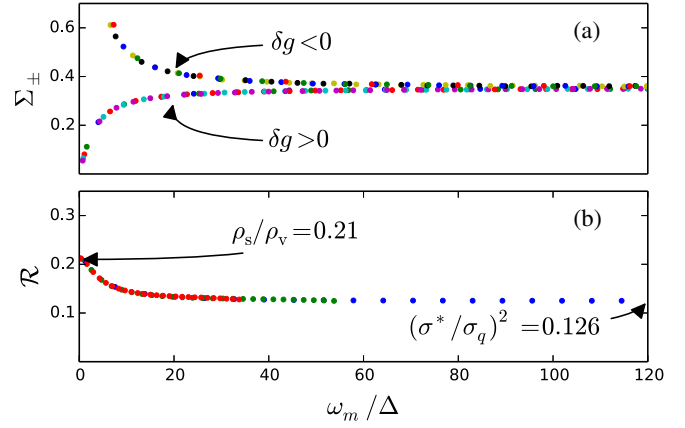


FIG. 3 (color online). (a) Scaling function of the dynamical conductivity in the superfluid ( $\delta g < 0$ ) and insulator ( $\delta g > 0$ ). Data for different values of the detuning  $\delta g$  collapse to two universal curves. (b) Measure of charge vortex duality of the  $O(2)$  model. Universal scaling function for  $\mathcal{R}(\omega_m)$  defined in Eq. (2). Deviation of this function from unity quantifies the difference between charge and vortex matter.

emergent Lorentz invariance [35], and hence, its critical properties are captured by the  $O(2)$  relativistic model in Eq. (5). We propose a direct approach to extract the capacitance of the Mott insulator using static measurements. In the insulator, the current and charge response functions are related by the continuity equation,  $\Pi_{xx}(k, \omega) = -(\omega^2/k^2)\chi_\rho(k, \omega)$ , where  $\chi_\rho(k, \omega)$  is the charge susceptibility. Hence,

$$C_{\text{ins}} = \lim_{\omega \rightarrow 0} \lim_{k \rightarrow 0} \frac{\Pi_{xx}(k, \omega)}{-\omega^2} = \lim_{k \rightarrow 0} \frac{\chi_\rho(k, \omega = 0)}{k^2}, \quad (13)$$

where the  $\omega \rightarrow 0$  and  $k \rightarrow 0$  limits commute since the insulator is gapped [36]. Thus, the capacitance is simply related to the finite  $k$  compressibility of the Mott insulator. This can be measured, e.g., by applying an optical potential at small wave vector  $k$  and probing the rearrangement of boson density using *in situ* imaging [37]. Temperature effects are discussed in the Supplemental Material [28].

Alternatively  $\sigma'(\omega)$ , for which experimental protocols were proposed, [11,38] can be used to compute  $\sigma''(\omega)$  by means of the Kramers-Kronig integral.

In summary, we computed the vortex condensate stiffness  $\rho_v$ , the high frequency universal conductivity, and provided a quantitative measure for deviation from self-duality as a function of Matsubara frequency. In addition, we suggest concrete experiments that test our predictions in THz spectroscopy of thin superconducting films and in cold atom systems.

We thank D. P. Arovas, M. Endres, A. Frydman, and W. Witczak-Krempa for helpful discussions. A. A. and D. P. acknowledge support from the Israel Science Foundation, the European Union under Grant No. IRG-276923, and the

U.S.-Israel Binational Science Foundation. We thank the Aspen Center for Physics, supported by Grant No. NSF-PHY-1066293, for its hospitality. S. G. acknowledges the Clore foundation for support.

- 
- [1] L. J. Geerligs, M. Peters, L. E. M. de Groot, A. Verbruggen, and J. E. Mooij, *Phys. Rev. Lett.* **63**, 326 (1989).
- [2] M. Köhl, H. Moritz, T. Stöferle, C. Schori, and T. Esslinger, *J. Low Temp. Phys.* **138**, 635 (2005).
- [3] I. B. Spielman, W. D. Phillips, and J. V. Porto, *Phys. Rev. Lett.* **98**, 080404 (2007).
- [4] M. Endres, T. Fukuhara, D. Pekker, M. Cheneau, P. Schau, C. Gross, E. Demler, S. Kuhr, and I. Bloch, *Nature (London)* **487**, 454 (2012).
- [5] A. M. Goldman, *Int. J. Mod. Phys. B* **24**, 4081 (2010), and references therein.
- [6] D. Sherman, B. Gorshunov, S. Poran, N. Trivedi, E. Farber, M. Dressel, and A. Frydman, *Phys. Rev. B* **89**, 035149 (2014).
- [7] S. Gazit, D. Podolsky, A. Auerbach, and D. P. Arovas, *Phys. Rev. B* **88**, 235108 (2013).
- [8] M. Swanson, Y. L. Loh, M. Randeria, and N. Trivedi, *Phys. Rev. X* **4**, 021007 (2014).
- [9] A. Raçon and N. Dupuis, *Phys. Rev. B* **89**, 180501 (2014).
- [10] W. Witzczak-Krempa, E. S. Sorensen, and S. Sachdev, *Nat. Phys.* **10**, 361 (2014).
- [11] K. Chen, L. Liu, Y. Deng, L. Pollet, and N. Prokof'ev, *Phys. Rev. Lett.* **112**, 030402 (2014).
- [12] E. Katz, S. Sachdev, E. S. Sorensen, and W. Witzczak-Krempa, *arXiv:1409.3841*.
- [13] M. P. A. Fisher and D. H. Lee, *Phys. Rev. B* **39**, 2756 (1989).
- [14] M. P. A. Fisher, G. Grinstein, and S. M. Girvin, *Phys. Rev. Lett.* **64**, 587 (1990).
- [15] M. E. Peskin, *Ann. Phys. (N.Y.)* **113**, 122 (1978).
- [16] C. Dasgupta and B. I. Halperin, *Phys. Rev. Lett.* **47**, 1556 (1981).
- [17] S. Gazit, D. Podolsky, and A. Auerbach, *Phys. Rev. Lett.* **110**, 140401 (2013).
- [18] Our conductivity is evaluated on both sides of the transition, see Supplemental Material [28].
- [19] A. Auerbach, D. P. Arovas, and S. Ghosh, *Phys. Rev. B* **74**, 064511 (2006).
- [20] D. Podolsky and S. Sachdev, *Phys. Rev. B* **86**, 054508 (2012).
- [21] D. Podolsky, A. Auerbach, and D. P. Arovas, *Phys. Rev. B* **84**, 174522 (2011).
- [22] K. Damle and S. Sachdev, *Phys. Rev. B* **56**, 8714 (1997).
- [23] N. Prokof'ev and B. Svistunov, *Phys. Rev. Lett.* **87**, 160601 (2001).
- [24] M. Hasenbusch and T. Török, *J. Phys. A* **32**, 6361 (1999).
- [25] M. E. Fisher, M. N. Barber, and D. Jasnow, *Phys. Rev. A* **8**, 1111 (1973).
- [26] E. Burovski, J. Machta, N. Prokof'ev, and B. Svistunov, *Phys. Rev. B* **74**, 132502 (2006).
- [27] E. L. Pollock and D. M. Ceperley, *Phys. Rev. B* **36**, 8343 (1987).
- [28] See Supplemental Material at <http://link.aps.org/supplemental/10.1103/PhysRevLett.113.240601>, for the finite size scaling analysis of the critical energy scales, the high frequency correction to scaling in Eq. (12) of the main text and the finite temperature effects on the capacitance in the insulating phase, which may prove useful for analysis of experimental data, which includes Refs. [10–12,22,27,29–31].
- [29] B. Capogrosso-Sansone, S. G. Söyler, N. Prokof'ev, and B. Svistunov, *Phys. Rev. A* **77**, 015602 (2008).
- [30] J. Cardy, *Scaling and Renormalization in Statistical Physics* (Cambridge University Press, Cambridge, England, 1996), Vol. 5.
- [31] M. Endres, Ph.D. thesis, Ludwig-Maximilians-Universität München, 2013.
- [32] J. Corson, R. Mallozzi, J. Orenstein, J. N. Eckstein, and I. Bozovic, *Nature (London)* **398**, 221 (1999).
- [33] R. W. Crane, N. P. Armitage, A. Johansson, G. Sambandamurthy, D. Shahar, and G. Grüner, *Phys. Rev. B* **75**, 094506 (2007).
- [34] A. Frydman (private communication).
- [35] M. P. A. Fisher, P. B. Weichman, G. Grinstein, and D. S. Fisher, *Phys. Rev. B* **40**, 546 (1989).
- [36] D. J. Scalapino, S. R. White, and S. Zhang, *Phys. Rev. B* **47**, 7995 (1993).
- [37] J. F. Sherson, C. Weitenberg, M. Endres, M. Cheneau, I. Bloch, and S. Kuhr, *Nature (London)* **467**, 68 (2010).
- [38] A. Tokuno and T. Giamarchi, *Phys. Rev. Lett.* **106**, 205301 (2011).